Nuclear Instruments and Methods in Physics Research B 125 (1997) 332–336

ELSEVIER

NIM B
Beam Interactions with Materials & Atoms

Multiple collisions in classical projectile–surface scattering

André Muis, J.R. Manson

Department of Physics and Astronomy, Clemson University, Clemson, SC 29634, USA

Abstract

A theoretical model of projectile–surface scattering which includes multiple collisions is developed using classical mechanical expressions for the single scattering of atomic-like particles from a many-body target. Explicit calculations are compared with two examples of recently measured experimental data: (i) 200 eV Na^+ ions reflected from Cu(001), and (ii) rare gas atoms in the eV energy range scattering from molten metals. We show that the classical equations for the scattering probability describe the observed intensities quite well when multiple scattering with several target atoms is included.

PACS: 79.20.Rf; 68.35.Ja; 03.65.Sq
Keywords: Photodesorption, Laser ablation, Thermal desorption

In many experiments involving the scattering of atomic, molecular or ionic projectiles from surfaces, over a range of incident energies from fractions of an eV to several hundred eV the back-scattered distribution is dominated mainly by deposition of energy and momentum into the vibrational modes and elementary electronic excitations of the target solid [1–4]. The initial and primary mechanism for this energy transfer is mechanical recoil scattering with the thermally vibrating surface target. Subsequently, the recoiling target atoms create a cloud of phonons or electron–hole pair excitations as they relax back into equilibrium with the target reservoir. In the classical limit, well-known expressions exist for describing the scattered intensity of an atomic-like projectile making a single classical collision with a thermally vibrating target [5–8].

In this paper we wish to consider the effects of multiple collisions of a projectile with a surface under classical scattering conditions. We use the classical scattering equations to develop a general multiple hit formalism based on the classical trajectories of the scattering projectiles. We apply this theoretical approach to the analysis of two recent experiments: scattering of a beam of incident energy E_i = 200 eV Na^+ ions from a Cu(001) surface [1], and scattering of beams of eV energy rare gas atoms from molten metal surfaces [2]. In both cases, multiple scattering events play a significant role in describing the scattered intensities. For the case of low-energy Na^+ ions scattering from the Cu(001) surface, the multiple scattering events were previously shown to give rise to distinct peaks in the scattered intensity, and our calculations agree well with the energy and temperature dependence of the measurements. For the rare gas scattering from liquid metals, the multiple collisions are shown to be important in extending the range of energy transfer, but do not give rise to distinct peaks in the measured spectrum. We also find that multiple scattering can account for the intensity at very low energies where one would expect thermal desorption of trapped gas atoms to be observed. This direct multiple scattering at low energies significantly reduces the estimates of the fraction of rare gas atoms that are captured at these incident energies.

In the classical limit, the single collision scattering of an atomic-like projectile from a surface at temperature T_S is completely solved in terms of closed-form analytic expressions. We express these in terms of the differential reflection coefficient $dR^{(1)}/d\Omega_f\,dE_f$ which gives the fraction of particles scattered into the small solid angle $d\Omega_f$ and into the small energy interval dE_f centered at the final energy E_f. For example, single collision scattering of an atomic projectile from a collection of discrete scattering centers is expressed as the following [5,6,8]:

$$\frac{dR^{(1)}}{d\Omega_f\,dE_f} = \frac{m^2|\boldsymbol{p}_f|}{8\pi^3\hbar^4 p_{iz}}\,|\tau_{fi}|^2\left(\frac{\pi}{\Delta E_0 k_B T_S}\right)^{1/2} \times \exp\left\{-\frac{(E_f - E_i + \Delta E_0)^2}{4k_B T_S \Delta E_0}\right\}, \qquad (1)$$

where $\boldsymbol{p}_q$ is the momentum of a particle in state q (which we will often write as $\boldsymbol{p}_q = (\boldsymbol{P}_q, p_{qz})$ with components parallel $\boldsymbol{P}_q$ and perpendicular p_{qz} to the surface), $|\tau_{fi}|^2$ is the form factor of the scattering center, m is the projectile mass, M_c is the crystal atom mass, and $\Delta E_0 = (\boldsymbol{p}_f - \boldsymbol{p}_i)^2/2M_c$ is the binary collision recoil energy.

Although Eq. (1) appears Gaussian-like in energy transfer $E_f - E_i$, the energy dependence of ΔE_0 can give rise to

0168-583X/97/$17.00
PII S0168-583X(96)00797-5

highly asymmetric peak shapes, for example under conditions in which $E_f \gg E_i$ the differential reflection coefficient becomes a decreasing exponential in E_f.

There is a somewhat different classical expression for the single collision scattering from a surface which can be considered as a flat continuous barrier [7–9]:

$$\frac{dR}{d\Omega_f\, dE_f} = \frac{m^2 v_R^2 |p_f|}{4\pi^3 \hbar^2 p_{iz} S_{u.c.}} |\tau_{fi}|^2 \left(\frac{\pi}{\Delta E_0 k_B T_S}\right)^{3/2} \times \exp\left\{-\frac{(E_f - E_i + \Delta E_0)^2 + 2v_R^2 P^2}{4k_B T_S \Delta E_0}\right\}, \quad (2)$$

where $\boldsymbol{P}$ is the parallel momentum exchange $\boldsymbol{P} = \boldsymbol{P}_f - \boldsymbol{P}_i$, $S_{u.c.}$ is the area of a surface unit cell, v_R is a weighted average of sound velocities parallel to the surface [7] and the term in the Gaussian-like exponent involving v_R and $\boldsymbol{P}$ arises from scattering from vibrational correlations at the surface. Typically, v_R is expected to be of the order of the Rayleigh velocity of the solid [7].

Eq. (1) applies to high-energy inelastic neutron scattering [5] as well as to ion scattering [10], while Eq. (2) has been shown to describe inelastic He–surface scattering at energies above 0.1 eV and for temperatures above room temperature [3]. In this latter case the flat continuous surface is the locus of classical turning points due to the Pauli exchange repulsion with the low-density surface electron distribution extending outward from the surface. These two distinct cases of Eq. (1) and (2) can be regarded as extreme limits. Eq. (2) describes a flat, uncorrugated surface, and Eq. (1) is for a highly corrugated surface in which the locus of classical turning points shrinks to small discrete spheres around the cores of the target atoms [11].

For incident conditions in which the differential reflection coefficient is nearly Gaussian in shape (high incident energies and small mass ratios $\mu = m/M_c < 1$), the characteristics of the scattered intensity are straightforward to describe. In this case the calculated peak position of Eq. (1) is very nearly given by the zero of the argument of the exponential, $E_f = E_i - \Delta E_0$. This is the classical recoil expression of Baule describing the situation in which the impulse momentum is deposited in a single stationary crystal atom and can be expressed, in terms of the total scattering angle $\theta = \pi - \theta_f - \theta_i$ as $E_f = f(\theta) E_i$ where

$$f(\theta) = \left(\frac{\sqrt{1 - \mu^2 \sin^2\theta} + \mu\cos\theta}{1 + \mu}\right)^2. \quad (3)$$

The same result holds for Eq. (2) when the term in P^2 in the exponent is small, which is usually the case when $V_R \lesssim 1000$ m/s.

The intensity at the point of most probable energy transfer is dictated by the envelope function which goes as

$$I_{MAX} \propto \frac{1}{(k_B T_S \Delta E_0)^{1/2}} \quad (4)$$

for the discrete case Eq. (1), and goes as $I_{MAX} \propto (k_B T_S \Delta E_0)^{-3/2}$ for the continuum case of Eq. (2). The characteristic power law exponent provides a clear signature difference between the two different limits.

The width of the energy distribution, as expressed in terms of the mean square deviation from the most probable energy, is given to a good approximation by

$$\langle \Delta E^2 \rangle \approx 2g(\theta) E_i k_B T_S, \quad (5)$$

where

$$g(\theta) = \frac{g_{TA}(\theta)}{\left(1 + \mu - \mu\cos\theta/\sqrt{f(\theta)}\right)^2}, \quad (6)$$

and where

$$g_{TA}(\theta) = \mu\left(1 + f(\theta) - 2\sqrt{f(\theta)}\cos\theta\right), \quad (7)$$

is the value taken by $g(\theta)$ in the trajectory approximation (TA). The trajectory approximation is obtained upon assuming that the recoil energy shift ΔE_0 appearing in the numerator of the argument of the exponential in Eq. (1) is constant, in which case $\langle \Delta E^2 \rangle \approx 2\Delta E_0 k_B T_S = 2g_{TA}(\theta) E_i k_B T_S$. For large scattering angles θ such as in the surface backscattering experiments discussed here, the narrowing of the intensity peak by the energy dependence of ΔE_0 is quite significant and the TA is a poor approximation [1].

Similar arguments hold for the peak widths given by Eq. (2) if v_R is small. If v_R is significant then Eq. (2) gives a peak which is further narrowed by the Gaussian-like term in the parallel momentum transfer $\boldsymbol{P}$. Another approximation which has often been used in surface scattering is the hard cubes model, which is based on the assumption that parallel momentum is conserved in the collision process, $\boldsymbol{P} = \boldsymbol{P}_f - \boldsymbol{P}_i \to 0$. This limit is obtained from Eq. (2) in the limit $v_R \to \infty$.

Multiple scattering, involving successive hits on different target atoms, is most simply expressed as a convolution of successive single-particle collisions. Through single plus double scattering terms, the multiple collision differential reflection coefficient is expressed explicitly as

$$\frac{dR^{(M)}(\boldsymbol{p}_f, \boldsymbol{p}_i)}{d\Omega_f\, dE_f} = \frac{dR_0^{(1)}(\boldsymbol{p}_f, \boldsymbol{p}_i)}{d\Omega_f\, dE_f} + \sum_{n=1}^{N} \int_0^\infty dE_q \times \int_{\Delta\Omega_n} d\Omega_q \frac{dR_n^{(1)}(\boldsymbol{p}_f, \boldsymbol{p}_q)}{d\Omega_f\, dE_f} \frac{dR_0^{(1)}(\boldsymbol{p}_q, \boldsymbol{p}_i)}{d\Omega_q\, dE_q} + \ldots, \quad (8)$$

where the summation runs over the set of target atoms with which second collisions can occur, and $\Delta\Omega_n$ is the solid angle subtended by the classical cross section of the nth atom. Higher-order multiple scattering terms can readily be added onto Eq. (8) as multiple convolutions of the single scattering differential reflection coefficient. For example, the

triple scattering would be the double convolution of three such terms:

$$\frac{dR^{(3)}(p_f,p_i)}{d\Omega_f\,dE_f}=\sum_{n'=1}^{N}\sum_{n=1}^{N}\int_0^\infty dE_q\int_{\Delta\Omega_n}d\Omega_q\frac{dR_n^{(1)}(p_f,p_q)}{d\Omega_f\,dE_f}$$
$$\times\int_0^\infty dE_{q'}\int_{\Delta\Omega_{n'}}d\Omega_{q'}\frac{dR_{n'}^{(1)}(p_q,p_{q'})}{d\Omega_q\,dE_q}\frac{dR_0^{(1)}(p_{q'},p_i)}{d\Omega_{q'}\,dE_{q'}}. \quad (9)$$

For the calculations below we have used Eq. (8) (together with Eq. (9) when required) with one further simplification. Since the solid angles subtended by the target atoms involved in the second collisions are usually small, we assume that the angular dependence of the intermediate differential reflection coefficients can be ignored, and the angular integration is replaced by a multiplicative factor of $\Delta\Omega_n$. Regardless of this simplifying approximation, the multiple scattering model depends on a single physical parameter, the classical cross section of the target atom which we usually express in terms of $\Delta\Omega/4\pi$, the fractional solid angle subtended by the cross section at the nearest-neighbor distance. Also, we take the form factor $|\tau_{fi}|^2$ to be a constant, which is appropriate for classical hard sphere scattering.

A recent and very precise set of experiments on the scattering of low energy ions from metal surfaces [1] provides an excellent test of the applicability of the classical scattering equations. Fig. 1 shows data at four different surface temperatures for the scattering of 200 eV Na^+ ions from a Cu(001) surface in the ⟨100⟩ azimuth with the incident and detector angles both at 45° from the normal. At each temperature three distinct peaks are observed and through classical trajectory simulations the individual peaks have been identified as due to either single or multiple scattering trajectories [1]. The peak with the largest energy loss (smallest final energy), which is also the dominant peak, is due to scattering from a single Cu atomic core. The peak at the largest final energy is due to double-forward scattering, i.e., successive collisions with two next-nearest-neighbor Cu cores in a straight line in the ⟨100⟩ azimuth. The middle peak at intermediate energy loss is assigned to two trajectories, a double scattering with adjacent neighbors in the forward ⟨110⟩ direction, and a triple scattering event first with the adjacent neighbor in the forward ⟨110⟩ direction and then with the next-nearest-neighbor in the forward ⟨100⟩ direction [1,12].

Our calculations using the multiple scattering formalism of Eqs. (8) and (9) with the discrete differential reflection coefficient of Eq. (1) are shown as dashed lines. For the multiple scattering we use the previously calculated trajectories [12]. In this case the large single scattering peak has no adjustable parameters and the multiple scattering peaks depend on the single parameter, the fractional solid angle subtended by a nearest neighbor Na/Cu cross section, which is chosen to be $\Delta\Omega/4\pi = 0.082$ in these calculations. This parameter value compares favorably with the simplest approximation for the fractional solid angle, given by the square of the ratio of the Cu atomic radius to the nearest-neighbor spacing $(1.57/2.55)^2/4 = 0.095$.

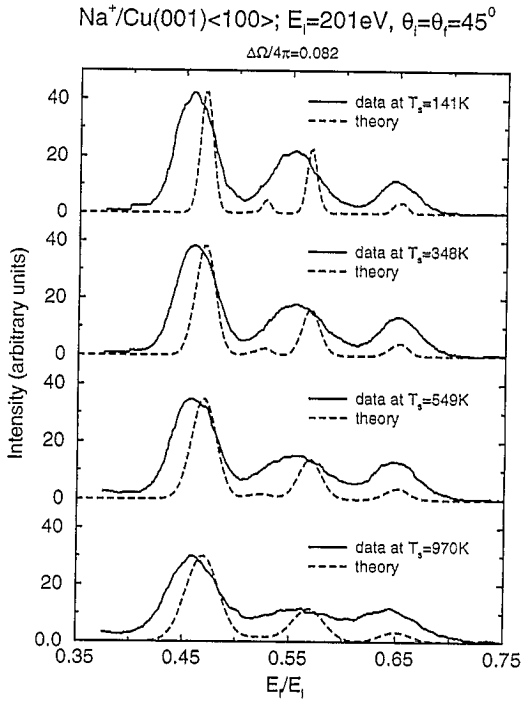

Fig. 1. Energy resolved intensity spectra plotted as a function of final particle energy for 201.2 eV Na^+ scattered from Cu(001)⟨100⟩ for four different surface temperatures with $\theta_i = \theta_f = 45°$. The solid lines are the experimental measurements [1] and the dashed lines are the calculations of Eq. (8) and (9). The large peak at lowest energy is due to single collisions, the peak at highest energy is due to double-forward scattering, and the peak in the data at intermediate energies is a combination of double and triple collisions. $\Delta\Omega/4\pi = 0.082$.

At the lowest temperature of 141 K the calculated single scattering and double-forward scattering peaks are positioned at slightly higher energies than the measurements, while the middle peak is distinctly separated into the following two features: one feature due to the out-of-line double scattering appearing at slightly higher final energy and the second feature due to the triple scattering which appears at slightly lower energy. The roughly 4% upward shift of the peak positions of the single scattering and double-forward scattering peaks can be made to coincide exactly with the measured peak positions with the addition of an approximately 10 eV deep attractive potential well representing the effects of the image force on the ion. As the surface temperature is increased all calculated peaks broaden. The triple scattering peak becomes relatively less important with T_S and this seems to explain the slight shift of the measured central peak toward higher final energies with increasing T_S.

Very careful and extensive measurements were made of the temperature dependence of the width of the single scat-

tering peak. It was found that in the range $100 < T_S < 950$ K the width consists of a temperature-independent constant term plus a term linear in temperature. The dependence of the width on surface temperature and on incident angle agrees quantitatively very well with Eq. (5) [1,10]. Some of the temperature-independent term can be ascribed to the natural isotopic mixture of Cu and to other experimental artifacts, while the remaining unexplained part may indicate temperature-independent energy losses to high-energy electronic excitations such as core-hole creation.

The overall temperature dependence of the peak intensities was not measured, thus we cannot compare directly with the relative theoretical dependence of the single scattering peak at different T_S implied by Eq. (4). However, the relative temperature dependence of the multiple collision peaks to that of the single collision peak is clearly in quite reasonable agreement with the calculations. The theoretical temperature dependence of all multiple scattering peaks is to a very good approximation the same as Eq. (4). Clearly, the results presented in Fig. 1 show that the overall features of the experimental data are well explained by the classical multiple collision scattering calculations presented here.

A second application of the classical multiple collision formalism presented here is a recent and very novel series of experiments on the scattering of monoenergetic beams with $E_i \approx 1$ eV of the rare gases Ne, Ar and Xe from the surfaces of the molten metals Ga, In and Bi [2]. Fig. 2 shows a series of three time-of-flight (TOF) spectra for a monoenergetic Ar beam of energy 0.95 eV incident on three different liquid metals: Ga and In at $T_S = 436$ K, and Bi at $T_S = 553$ K. The incident and detector angles are both at 55° with respect to the surface normal. A single broad peak with a long tail at small final energies (large times) is evident in all spectra. The single collision calculations based on the differential reflection coefficient of Eq. (1) are shown as a short-dashed line, the double collision contribution as a long-dashed line, and the total single plus double collision calculation as the dash–dotted line.

The double collision contributions in this calculation were obtained by taking the average over all in-plane orientations of a distribution of six nearest neighbors in hexagonal symmetry, each subtending the same fractional solid angle $\Delta\Omega/4\pi$. In all three cases the multiple collision model agrees very well with the measured intensities. In agreement with the scattering of higher energy Na^+ ions, the double-forward scattering contributes strongly to the total multiple collision contribution. However, an important contribution also comes from the double-backward scattering, i.e., those scattering events in which the rare gas atom scatters backwards in the surface plane after the initial collision with a liquid metal atom, and subsequently suffers another large angle scattering event which projects it forward again into the detector direction. These double-backward events result in large energy losses for the projectile and are the reason for the relatively strong intensity at large TOF times in the multiple scattering contribution. For Ar scattering from Ga,

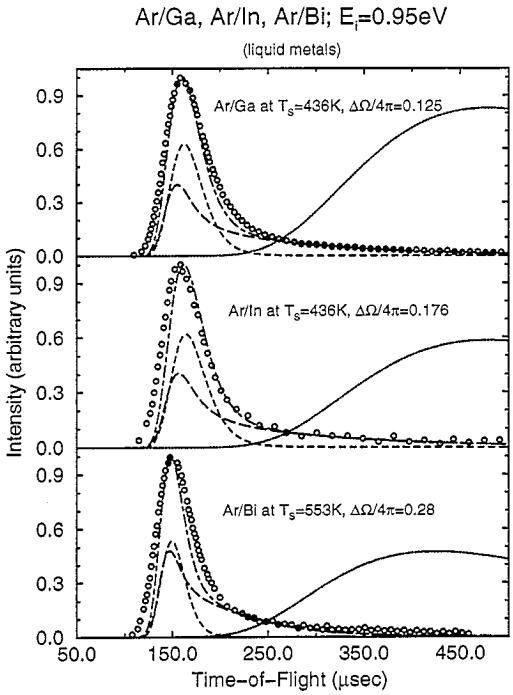

Fig. 2. A series of time-of-flight spectra for a 0.95 eV incident Ar beam on the three liquid metals Ga and In at T_S = 436 K and Bi at T_S = 553 K. The experimental points are shown as circles (o) [2]. The theoretical curves are: (i) short-dashed, single collisions only; (ii) long-dashed, only double collisions with all nearest neighbors; and (iii) dash-dotted, single plus double collisions. For Ar/Ga scattering an effective target mass of 1.75 Ga masses was used. In all cases there is negligible evidence for appreciable capture and subsequent thermal desorption, as can be seen from the Maxwellian desorption curve for the temperature T_S which peaks at much lower energies.

which has the smallest mass of the three metals, the position of the maximum in the TOF peak implies a collective mass effect in the surface [2]. In order to obtain the agreement between theory and measurement shown in Fig. 2 we used an effective mass for Ga equal to 1.75 Ga masses. For the other two metals no mass correction was necessary. The values of $\Delta\Omega/4\pi$ used in the calculations are shown in Fig. 2, and in all cases they are relatively close to the values expected from geometrical considerations based on the average interatomic distance in the liquid and the atomic radii of the cores. It is interesting to note that the good agreement of the multiple collision calculations with the data at small final energies indicates that there is very little trapping or capture of the Ar with subsequent thermal desorption. There is no significant peak in the data near the position of the expected thermal desorption maximum at large TOF times, which is indicated by the (flux corrected) Maxwellian distribution curves, and the intensity in the low-energy tail appears to be well explained by the multiple scattering calculations.

Additional experimental results are presented in Fig. 3, which show scattering from a liquid In surface by beams of the three rare gases Ne, Ar and Xe at the incident energies

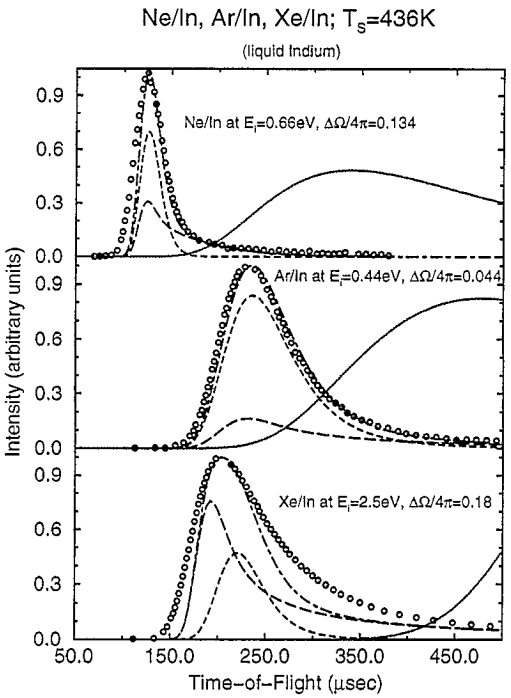

Fig. 3. Ne, Ar and Xe scattering from liquid In at T_S = 436 K with incident energies as marked. The experimental data are shown as circles (○) [2]. The theoretical curves are the same as in Fig. 2: (i) short-dashed, single collisions only; (ii) long-dashed, only double collisions with all nearest neighbors; and (iii) dash-dotted, single plus double collisions. For Xe an effective target mass of 2.0 In masses was used. Again, there is no significant evidence for a thermal desorption signal.

indicated. The incident and detector angles are the same as in Fig. 2, as are the calculated curves. Again, the multiple collision calculations are in good agreement with the measured TOF spectra. The Xe/In data provide an interesting case because Xe is more massive than In and hence a single binary collision with a stationary In atom cannot back-scatter Xe into the detector direction. However, back-scattering of Xe is possible in the present surface scattering experiments, both because of the initial thermal motion of the In atoms and through multiple collisions. For the calculations shown for Xe in Fig. 3, in order to obtain agreement with the position of the maximum in the TOF peak, it was necessary to use a collective mass for In which is 2.0 times the atomic mass of In. This appears to be additional evidence that in the case of large mass projectiles and small mass target atoms, collective mass effects are not negligible. For the case of Ar and Ne on In a collective surface mass was not needed, and the atomic mass of In was used for those calculations.

The comparisons with experiment presented here show that the classical expressions for the scattering probabilities, with the added contributions of multiple collisions, do a reasonable job of describing the observed scattering intensities for a large class of systems and over a wide range of temperatures and incident energies. These classical equations provide a fundamental framework for predicting the major mechanisms of energy losses to the vibrational and low-energy electron–hole pair excitations of the thermal surface reservoir in projectile–surface collisions.

Acknowledgements

This work was supported by the NSF under Grant DMR 9419427.

References

[1] C.A. DiRubio, D.M. Goodstein, B.H. Cooper and K. Burke, Phys. Rev. Lett. 73 (1994) 2768.
[2] W.R. Ronk, D.V. Kowalski, M. Manning and G.M. Nathanson, J. Chem. Phys. 104 (1996) 4842.
[3] F. Hofmann, J.R. Manson and J.P. Toennies, Surf. Sci. 349 (1996) L184.
[4] J.A. Barker and C.T. Rettner, J. Chem. Phys. 97 (1992) 5844; J.A. Barker and D.J. Auerbach, Surf. Sci. Rep. 4 (1984) 1.
[5] A. Sjölander, Ark. Fys. 14 (1959) 315.
[6] D.A. Micha, J. Chem. Phys. 74 (1981) 2054.
[7] R. Brako and D.M. Newns, Phys. Rev. Lett. 48 (1982) 1859; Surf. Sci. 123 (1982) 439.
[8] J.R. Manson, Phys. Rev. B 43 (1991) 6924.
[9] H.-D. Meyer and R.D. Levine, Chem. Phys. 85 (1984) 189.
[10] A. Muis and J.R. Manson, Phys. Rev. B 54 (1996) 2205.
[11] J.R. Manson, to be published.
[12] C.A. DiRubio, Ph.D. thesis, Cornell University (1993).